Int Nano Lett
DOI 10.1007/s40089-017-0211-5

ORIGINAL ARTICLE

Dye-modified ZnO nanohybrids: optical properties of the potential solar cell nanocomposites

Wasiu B. Ayinde[1,2,8] · Enock O. Dare[1,4] · Damilola A. Bada[1] · Samson O. Alayande[1,3] · Fatai O. Oladoyinbo[1] · Mopelola A. Idowu[1] · Bukola. O. Bolaji[5] · Miriam I. Ezeh[6] · Rose U. Osuji[7]

Received: 7 August 2015 / Accepted: 17 June 2017

Abstract We report the hybridization of ZnO with natural dyes [Laali, Zobo] or synthetic dye [methyl red] forming ZnO–laali, ZnO–zobo and ZnO–methyl red nanocomposites in bright colours. The structural, optical and dye photosensitization influence of the hybrid nanocomposites were studied by X-ray diffraction (XRD), scanning electron microscope (SEM), UV–Visible absorption spectroscopy and photoluminescence (PL). The surface plasmon absorption band of ZnO–laali and ZnO–zobo shifts towards red and blue, respectively, with significantly enhanced absorption intensities, indicating the interaction and optical influence of the respective dyes in photosensitization. Optical and absorption character of ZnO methyl red and bare ZnO are similar indicating the insignificant effect of methyl red on photosensitization. PL spectra of ZnO–laali and ZnO–zobo display enhanced UV light emission due not only to the surface electron transfer from their respective inherent isoplumbagin and anthocyanin to ZnO but also to the extension of the Fermi energy level to the ZnO. Dyes adopted influence the optical band gaps of the evolved hybrid nanocomposites.

Keywords Zinc oxide nanohybrids · Natural dyes · (Zobo) *Hibiscus sabdariffa* · (Laali bark) *Lawsonia inermis* · Optical properties

Introduction

Nanosized particles of semiconductor materials have gained much more interest in recent years due to their desirable properties and applications in different areas such

✉ Wasiu B. Ayinde
twasiu33@gmail.com

✉ Enock O. Dare
dare3160@hotmail.com

Damilola A. Bada
dammexonline@gmail.com

Samson O. Alayande
gbengaalayande@gmail.com

Fatai O. Oladoyinbo
oladoyinbofo@funaab.edu.ng

Mopelola A. Idowu
Maidowu408@yahoo.com

Bukola. O. Bolaji
bukola.bolaji@fuoye.edu.ng

Miriam I. Ezeh
ezehmiriam@gmail.com

Rose U. Osuji
uzosuji@yahoo.com

[1] Department of Chemistry, Federal University of Agriculture, Abeokuta, Nigeria

[2] Prototype Engineering Development Agency, PMB 5025, Ilesa, Osun State, Nigeria

[3] Center for Energy Research and Development, Obafemi Awolowo University, Ile-Ife, Nigeria

[4] Nanosciences Laboratories, Materials Research Department, iThemba LABS, Somerset West 7129, South Africa

[5] Department of Mechanical Engineering, Faculty of Engineering, Federal University Oye-Ekiti, Ikole Campus, PMB 373, Oye-Ekiti, Ekiti State, Nigeria

[6] Department of Physics, Delta State University, Abraka, Nigeria

[7] Department of Physic and Astronomy, University of Nigeria, Nssuka, Nigeria

[8] Department of Ecology and Resource Management, School of Environmental Science, University of Venda, Thohoyandou, Private Bag X5050, Limpopo, South Africa

Published online: 28 June 2017

as catalysts, [1] sensors, [2] photoelectron devices [3, 4], and highly functional and effective devices [5]. These nanomaterials have novel electronic, structural, and thermal properties which are of high scientific interest in basic and applied fields. Zinc oxide (ZnO) is a wide band gap semiconductor with an energy gap of 3.37 eV at room temperature. It has been used considerably due to its catalytic, electrical, optoelectronic, and photochemical properties [4, 6, 7]. ZnO nanostructures have a great advantage when applied to catalytic reaction process. This is due to their large surface area and high catalytic activity [8]. The excellent optical properties of ZnO have made it a useful semiconductor in Dye-Sensitised Solar Cell (DSSC); a third generation photovoltaic device that holds a significant promise for the inexpensive conversion of solar energy to electrical energy.

The use of dye sensitization in photovoltaics has received a great interest after the breakthrough achieved by Grätzel et al. [9], in the early 1990s. They developed a DSSC with energy conversion efficiency exceeding 7% in 1991 [5] and 11.4% in 2001 [10] by combining nanostructured electrodes to efficient charge injection dyes. Since then, TiO_2 nano-particle films have been widely investigated for DSSCs. However, TiO_2 films have some defects such as lack of enough energy barriers between the interface of the films and electrolytes. The existence of plenty of electron-trapped surface states is the cause of the re-combination [11]. The photo-catalytic activity of TiO_2 is so high under the UV radiation of natural sun-light that organic materials in DSSCs may decompose during outdoor use, resulting in long-term reliability problems for the conversion efficiency. Hence, some investigations have been turned to ZnO films, which have a much lower photocatalytic activity and less electron-trapped surface states [12]. It has been reported that ZnO performs particularly well when sensitised with organic dyes [13]. However, in spite of its synthesis simplicity and promising industrial value, ZnO/dye-sensitised solar cell is still far below the TiO_2/dye cell which is more expensive to produce. Consequently, a lot of activity has been exercised of late to enhance the performance of ZnO/dye solar cell.

The dye that is used as a photosensitizer plays an important role in the operation of DSSCs. The function of dye is to absorb light, inject electrons from the redox mediator. Light harvesting dyes absorb solar radiation incident which results in the excitation of molecules, which pass the energy obtained by means of transferring electrons onto a nanocrystalline semiconductor substrate onto which they are adsorbed. The efficiency of the cell is critically dependent on the absorption spectrum of the dye and its anchorage on the surface of the semiconductor. Much work has concentrated on organic dyes and organic metal complexes. On the other hand, natural dyes extracted from fruits and flowers have attracted the attention of many researchers [14], and many natural dyes have been proven to be efficient dyes as photo-sensitizers in DSSCs. Natural dye is readily available and cheap, thus, making it environmental friendly with potential capacity to reduce the cost of DSSC devices. In particular, Laali, as popularly called, is grown in the savannah region of West Africa [15] and are used as colouring material in the designing of fashionable tattoos on human bodies. *Lawsonia inermis* (Laali) is a very popular natural dye used in colouring fingers, hands, nails and hair (in northern part of Nigeria). The pyhtochemical mainly found in Laali stem bark is called Isoplumbagin. Zobo (*Hibiscus sabdarifa*) richly contains anthocyanin pigment, and is responsible for its red or wine colour depending on whether it has structural attachment of glucose or not [16]. Cyanidin-3-glucoside is a member of anthocyanin family [17].

In this work, ZnO–laali, ZnO–zobo or ZnO–methyl red was prepared for the purpose of an enhanced optical properties and photosensitization. In view of the limitation of inorganic solids, organic additives certainly play a crucial role in boosting electro-optical speed of DSSC. Methyl red, a photo-sensitive dichroic dye has also been considered in comparison with Laali and Zobo to photosensitize ZnO for enhanced optical properties.

Experimental

Materials

Zinc nitrate hexahydrate, $Zn(NO_3)_2{\cdot}6H_2O$, methyl red and ethanol were commercially procured. Sodium hydroxide, NaOH was obtained from FUNAAB laboratory. All chemicals were of analytical grade unless otherwise stated.

Natural dye extraction

Preparation of Lawsonia inermis 'Laali' extract

Laali dye was extracted as described by Adenike et al. [18]. Fresh Laali stem barks were collected at Lemomu Ayeni Street, Oluwo-Onikolobo, Abeokuta, Ogun State, Nigeria. The Laali barks were washed with distilled water and dried at 60 °C in the oven. Laboratory ceramic made mortar and pestle were used to crush the dried sample. 20 g of the dried sample was weighed and soaked in 200 mL solution of ethanol. This was left to age at room temperature in a dark place for 24 h. The solid residues were filtered out to obtain a clear greenish solution which was concentrated in a rotary evaporator.

Preparation of Hibiscus sabdariffa (zobo) extract

The *Hibiscus sabdariffa* (*Zobo*) dye was extracted according to literature method [19]. Dried succulent red calyxes of (*Hibiscus sabdariffa*) were purchased from the market, washed, air-dried and grinded to powdery form using mortar and pestle. 20 g of the ground sample was then soaked in 200 mL distilled water for about 24 h. After extraction, the solution was filtered to obtain a clear wine colour.

The solution was then concentrated in a rotary evaporator. To prevent darkening, the concentrate obtained was stored in amber-coloured bottle.

Preparation of ZnO–dye

ZnO–methyl red dye

ZnO–methyl dye was prepared according to Taher et al. [20] with some slight modifications. 14.4 g Zinc nitrate hexahydrate was dissolved in 100 mL of ethanol under stirring at room temperature. Simultaneously, the prepared 0.36 M sodium hydroxide solution was added drop-wise. The solution was then sealed at this condition for 1 h.

0.25 g of powdered methyl red dye was dissolved in 100 mL of ethanol. 1.0 mL of this solution was added to white ZnO Nanoparticles (ZnO Nps) drop-wisely while the stirring continued for another 1 h. It was observed that the whole solution changed from white to pink at this point. The ZnO–methyl red dye solution was allowed to settle overnight. The supernatant solution was separated carefully. The remaining solution was centrifuged for 10 min and the precipitate was removed. The precipitated ZnO–methyl red dye solution was washed three times with distilled water and ethanol and then dried in the oven at about 80 °C. The resulting ZnO–methyl dye composite was then examined in terms of structural, chemical and optical properties [20].

ZnO–zobo (Hibiscus sabdarifa) dye nanocomposite

1.0 mL of concentrated *Hibiscus sabdariffa* extract was added to the stirring suspension of ZnO particles. It was observed that the whole solution turned blue and stirring continued for another 1 h. The ZnO–zobo dye solution was allowed to settle overnight. The supernatant solution was separated carefully. The remaining solution was centrifuged for 10 min, and the precipitate was removed. The precipitated ZnO–zobo dye solution was cleaned three times with distilled water and ethanol and then dried in the ovum at about 80 °C. The resulting ZnO–zobo nanopowder was then examined in terms of structural, chemical and optical properties.

ZnO–laali (Lawsonia inermis) dye nanocomposite

ZnO–*Lawsonia inermis (Laali)* dye nanocomposite was prepared in a similar way as ZnO–*zobo* nanocomposite except that 1.0 mL of *Laali* was added instead of *Hibiscus sabdariffa.* In the third step, the colour changed from white to very light green.

The resulting ZnO–*laali* dye nanopowder was then examined in terms of structural, chemical and optical properties.

Desorption and re-adsorption experiment

To examine the nature of surface attachment of dyes onto ZnO, dye-desorption experiment was carried out by adding the coloured hybrid ZnO–dye nanocomposite into KOH (pH 10.5) and stirred for 2 h. Colour of the resulting nanocrystal was observed and subjected to UV–Vis analysis. The dye was re-adsorbed onto the resultant nanocrystals following the same experiments as outlined in 2.2.

Characterization

The morphology, size distribution and the elemental composition of the nanocomposites were determined by scanning electron microscopy, SEM [JEOL/EO (version 1.0) (JEOL Ltd, Tokyo, Japan)] along with Energy Dispersive X-ray Spectroscopy (EDS) and JEOL 1010 TEM with an accelerating voltage of 100 kV. Crystallinity and phase purity of the materials were determined by X-ray diffraction (XRD) recorded at room temperature using X-ray diffractometer (ARL X'TRA) with Cu-K_α radiation (wavelength: 0.15405 nm). Data were collected in the range from $2\theta = 10°$–$90°$. Optical measurements were taken using UV–Vis absorption (T60 UV–Vis spectrophotometer) and Photoluminescence LS50 fluorescence spectrometer. EDS, XRD, UV–Visible spectra and SEM results were obtained from Sheda Science and Technology Complex (SHESTCO), FCT, Abuja, Nigeria and iThemba laboratory, Somerset west, South Africa.

Results and discussion

Hybridization of ZnO with the selected dyes was carried out with evidence of colour changes which signified adsorption inside or outside of the ZnO. The white ZnO changed colour when dye was adsorbed.

Figure 1 indicates the SEM images of (a) ZnO–laali, (b) ZnO–methyl red and (c) ZnO–zobo as it corresponds to their respective (top) structural reaction scheme patterns. SEM image 1a corresponding to ZnO–laali reflects an

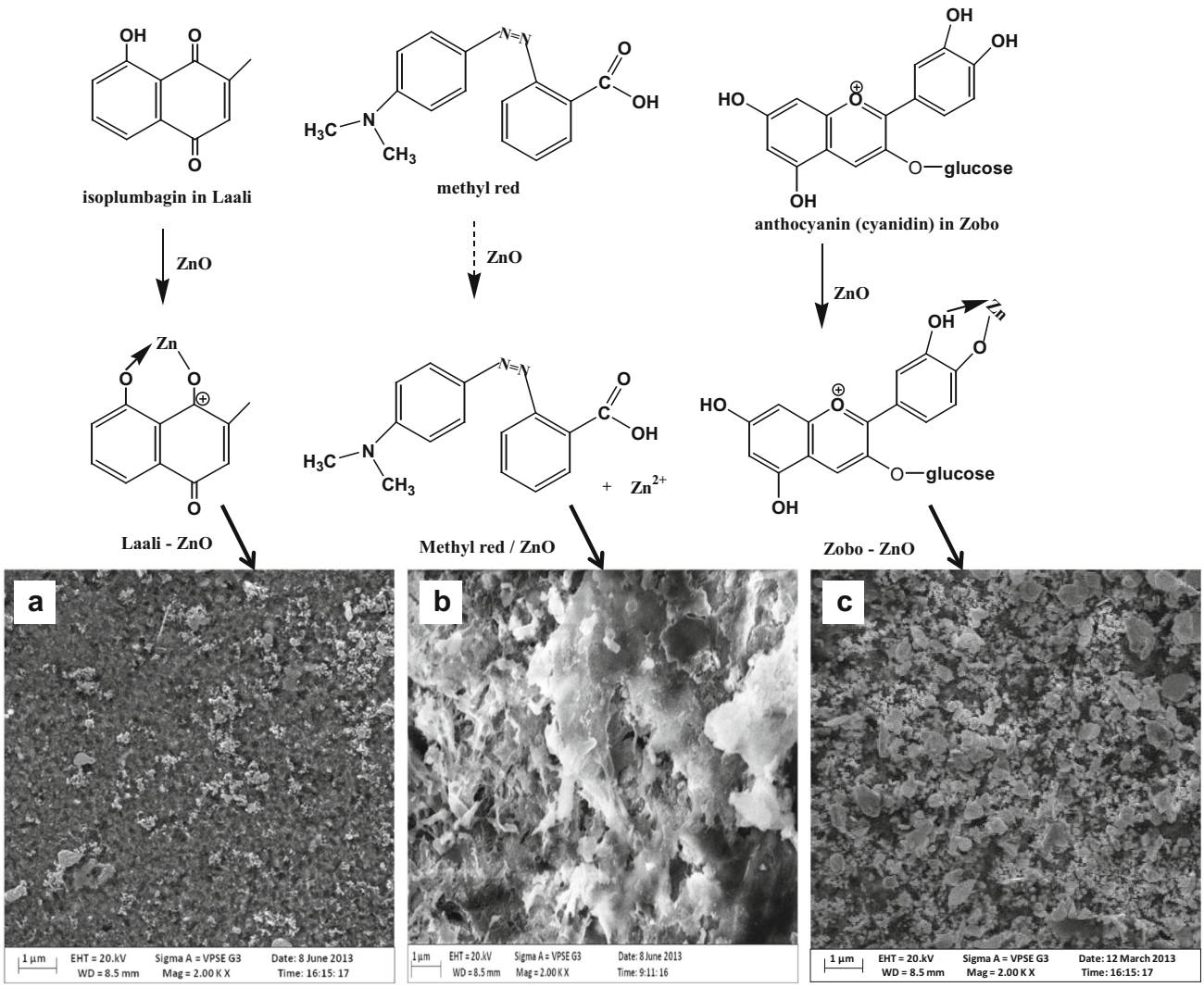

Fig. 1 *Top* Scheme of interaction between Laali (isoplumbagin), methyl red or Zobo (anthocyanin) and ZnO nanoparticles and their corresponding SEM images (*bottom*) **a** Laali–ZnO, **b** methyl red/ZnO, **c** Zobo–ZnO

orderly, well-dispersed and uniformly dyed nanocomposite. This shows that isoplumbagin in Laali is fully anchored on ZnO surface with a likely complexation reaction as schematically represented. Similar structural behaviour is shown in Fig. 1c for ZnO–zobo. Zobo contains cyaniding-3-glucoside, which is a member of anthocyanin isolated natural dye that is equally found in blackberries [21] and red cabbage [22]. Uniformly distributed anthocyanin-dyed ZnO as seen in a well-dispersed image (Fig. 1c) is also an evidence of complexation between cyaniding-3-glucoside and Zn ion.

Buraidah et al. [23] reported anthocyanin dye extract from red cabbage as sensitization to semiconductor for solar cells. The cyanidin glucoside effectively formed a complex with TiO_2 particles. The hydroxyl group in cyaniding molecule has been found to effectively bind to the surface of TiO_2 as proposed by Hao and co-workers. On the contrary, Fig. 1b which represents ZnO–methyl red image displays excessive agglomerates in the form of "splash of dye" on ZnO surfaces. This means that the surface binding of –COOH of methyl red is limited by its stability, resulting into insufficient dye adsorption because of the acidic nature of the dye [24].

A clearer view of ZnO–dye composite morphology is as shown in the TEM of Fig. 2. The morphology is a multiply-twin structure which indicates Laali-capped ZnO. This result signals Laali dye anchoring on ZnO. There was no intimate association of dye within ZnO matrix. To evaluate the stability status of the nanocomposite, TEM images were taken at different time intervals. There was no significant change in the morphology of Laali-capped ZnO after 12 months when compared with the one previously taken after 2 months of synthesis. This is an indication of stability as displayed by the nanocomposites.

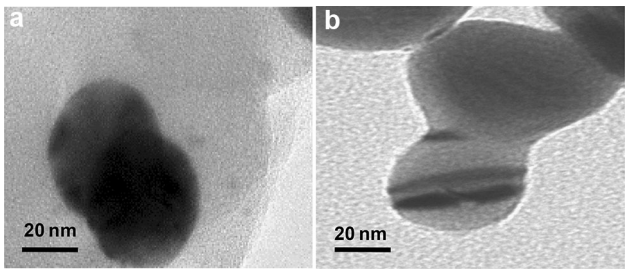

Fig. 2 TEM images of ZnO–laali nanocomposite **a** after 2 months, **b** after 12 months

Table 1 Absorbance data for dye desorption and dye readsorption onto ZnO

ZnO–dye	Desorption		Re-adsorption	
	Wavelength (nm)	Intensity	Wavelength (nm)	Intensity
ZnO–laali	350	0.36	352	0.39
ZnO–methyl red	341	0.08	340	0.18
	534	1.4		
ZnO–zobo	343	0.19	344	0.22

Dye-desorption and re-adsorption [25] experiments were carried out to evaluate the effectiveness and nature of surface adsorption of Laali, methyl red or Zobo unto ZnO surfaces. The experiments were carried out while stirring ZnO–laali, ZnO/methyl red or ZnO–zobo in KOH solution at pH 10.5 and reruns of UV–Vis of the dye-desorbed and -re-adsorbed ZnO. Summary of the resulting absorption data of the "re-adsorbed" and "desorbed" system are found in Table 1.

For ZnO–laali, the absorbance intensities recorded for desorption (0.36) and re-adsorption (0.39) are in a very close range at almost the same wavelength. KOH did not influence the dislodgement of dye from ZnO. These results signify a strong bond between isoplumbagin and ZnO surface which implies that the dye was adsorbed at the crystalline phases of ZnO. Similar trends are observed in the case of ZnO–zobo implying strong bond and adequate coverage of ZnO surfaces in and out with anthocyanin dye. The strong bond, unaffected by KOH, is an evidence of complexation between the respective active components of the dyes and ZnO. These results have been corroborated with SEM images. On the contrary, KOH strongly influenced structural connectivity between methyl red and ZnO causing a distinct separation between them and eventual bimodal absorbance bands assignable to methyl red (534 nm) and ZnO (341 nm). Methyl red on its own has a unique high intensity (1.4) at wavelength 534 nm which conforms with the report [23]. Evidence of dye disengagement is seen in the relative intensities of the desorbed

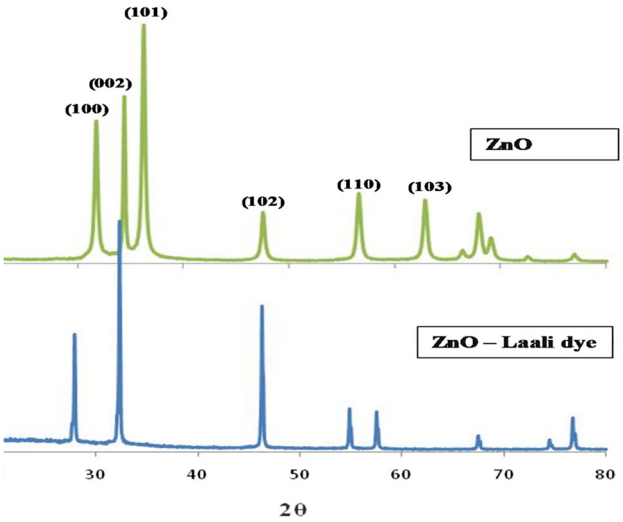

Fig. 3 XRD patterns for ZnO and ZnO–laali dye

(0.08) and re-adsorbed (0.18). However, the intensity of the desorbed methyl red from ZnO surface is distinctively lower when compared with the desorption of anthocyanin or Zobo from ZnO. These results further serve as clarification that methyl red did not sensitise ZnO because of the unreactive nature of the acidic dye and agglomerates formation which limits electron injection from the dye to ZnO. Indeed, there is clear evidence from the absorbance intensities that Laali and Zobo possess reasonable character of dye-sensitising agent as the dye re-adsorption absorbance intensities are close to desorption counterpart.

Figure 3 shows the XRD patterns of as-synthesised ZnO and ZnO–laali. For comparison, the XRD pattern for ZnO–laali was changed at peak position (100) and (002), which shifted towards smaller angle θ and displayed relatively smaller and higher diffraction intensities, respectively when compared with that of ZnO.

However, peak position (101) is completely absent in the ZnO–laali spectrum. The shift of the characteristic prominent peaks diffraction angle towards the lower 2θ increases in diffraction intensities at (002), (102) and the absence of (101) indicates an evidence of ZnO–Laali dye coexistence and its formation in a single motif. This account for the gradual loss of crystallinity as dye is anchored predominantly on the (002), (101) and (102) crystalline phases. Hence, incorporation of the dye via complexation reaction between isoplumbagin of the dye molecule and Zn^{2+} caused considerable distortion of the ZnO lattice and stress at the interface between ZnO and Laali dye. The consequence of this stressful scenario resulted in shifting of various peak position of planes leading to suppression along the (101) face [24].

It is worth of note that no significant difference was noted on the XRD spectra of ZnO when compared with that

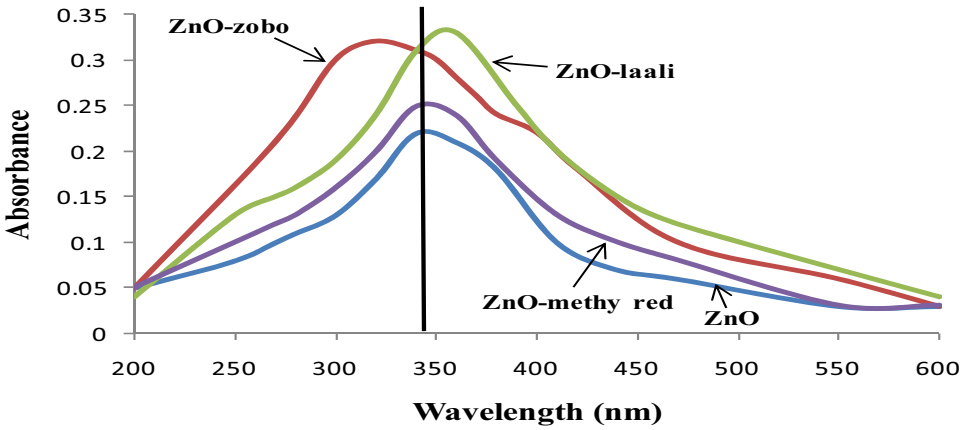

Fig. 4 The UV–Vis absorption spectra of ZnO, ZnO–methyl red, ZnO–zobo and ZnO–laali

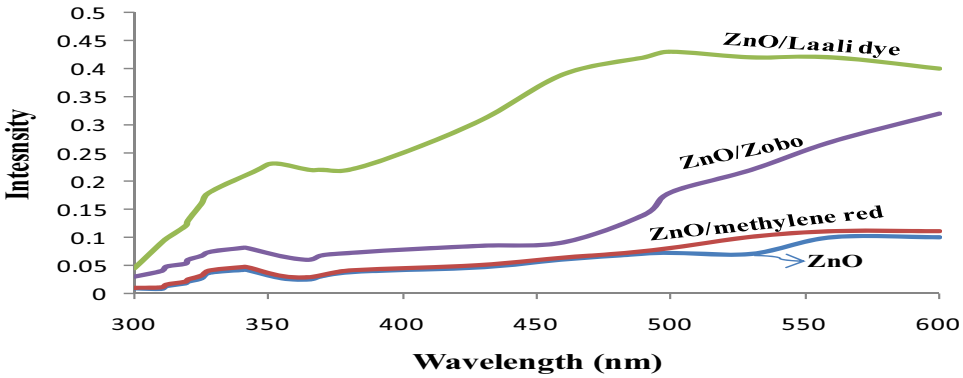

Fig. 5 Photoluminescence (PL) spectra of ZnO, ZnO–methylene red, ZnO–zobo and ZnO–laali nanocomposites

of ZnO–methyl red and ZnO–zobo. Expectedly, XRD of ZnO–zobo should behave similar to that of ZnO–laali. Further explanation is required to support this anomaly.

The optical properties of ZnO, ZnO–laali, ZnO–zobo and ZnO–methyl red were evaluated by UV–Vis absorption spectroscopy and Photoluminescence (PL) spectroscopy. Apparently, ZnO and ZnO–methyl red exhibits single absorption peaks at around 340 nm on the UV–Vis spectra (Fig. 4). This result suggests that methyl red dye did not significantly influence the optical and absorption characteristic of the composite as it behaves almost akin to unhybridized ZnO, however, with a slight increase in intensity due to ZnO in dye environment.

The result has been corroborated with SEM image result displaying a splash of dye around ZnO with no evidence of ZnO/methyl red intermixing. The limited ZnO–methyl absorption performance may be explained by the instability of ZnO in acidic dyes, which implies that methyl red caused the dissolution of Zn atoms at ZnO surface, resulting in the slow electron-injection kinetic from methyl red to ZnO [24].

ZnO–laali and ZnO–zobo displays exceedingly higher absorption and optical characteristics when compared with ZnO and ZnO–methylene red. ZnO–laali is red shifted with increased absorption intensity higher than all other nanocomposites. ZnO–zobo is blue shifted with reasonable absorption intensity. The shift is quite distinctively different from reported absorption spectrum of extracted anthocyanin dye which is found at $\lambda = 535$ nm [23]. The ascending increasing order of absorption intensities (ZnO–laali > ZnO–zobo > ZnO–methylene red >ZnO) is an indication of optical influence of various dyes which enhances photosensitization of ZnO. Red shifting is observed in the case of ZnO–laali as evident in an increased particle size (8.3 nm) as determined from the FWHM of the main intensity peak ($2\theta = 32.25°$) using Debye–Scherrer's equation. The average particle size of the ZnO was found to be 6.5 nm which was derived from the FWHM of the main intensity peak corresponding to (101) at 36.33° while that of ZnO–methyl red was found to be 6.3 nm. The close range in sizes of both ZnO and ZnO–methylene red suggests that the dye and ZnO in the composite are not in a single motif, confirming ZnO/methyl red unreactivity. ZnO–zobo has a reduced particle size (7.8 nm) when compare with ZnO–laali. The distinctive broadening, red shifting and enhanced intensity of ZnO–laali could be due to stronger interfacial complexation between isoplumbagin of the dye molecule and ZnO leading to electron transfer from the dye to ZnO.

The photoluminescent (PL) optical characteristics of the nanocomposites are presented in Fig. 5. The PL spectrum

of each sample indicates two emission bands in the UV/visible range.

The UV emission band display at 344 nm in all composites is attributed to the radiative recombination occurring in the ZnO. Furthermore, it can be seen that ZnO–laali and ZnO–zobo exhibit additional weak peak around 502 and 495 nm, respectively, giving two prominent peaks on each spectrum. These two weak bands are found to be red shifted and with higher intensity relative to the excitonic emission peak of ZnO nanostructure found at 344 nm. The intensity of the ZnO radiative recombination in ZnO–laali is with the highest intensity and is followed by ZnO–zobo. The observed intensities in the cases of ZnO and ZnO–methyl red are the same in overlapping style, suggesting insignificant effect of dye on the optical performance of the later. Under the irradiation of incident light having a wavelength larger than the particle size, the high-density electron of the active dye molecules form an electron cloud and oscillate. As Laali or Zobo molecule complexed with Zn^{2+}, the electron accumulates at the interface between the dye and ZnO, leading to the downward band bending of the ZnO side and thus to the easy electron transfer from Laali, in particular, to the ZnO side [26].

Figure 6 plausibly represent the band bending Fermi energy of the ZnO and electron transfer from Laali dye to the ZnO.

The UV light emission intensity of the Zn–laali dye is observed as the highest peak distinctively. The reason for this is also due to the fact that, under this analogy, light scattering is stronger than absorption leading to efficient transfer of electron from Laali dye to ZnO as further provided in the literature [26] based on Rayleigh theory [27].

The optical band gap of the ZnO–dye composites were determined using well established Tauc model [28] represented by the following equation: $\alpha h\upsilon = B(h\upsilon - \mathrm{Eg})^{1/2}$, where h is the Planck's constant, υ is the frequency of the incident photons and B indicates a constant that depends on the electron–hole mobility. Figure 7 shows the plots of $(\alpha h\upsilon)^2$ against photon energy ($h\upsilon$) for ZnO, ZnO–laali dye, ZnO–zobo dye and ZnO–methyl red with optical band gaps found to be 3.7, 3.1, 4.3 and 4.0 eV, respectively.

These results clearly indicate that optical band gaps of the ZnO nanocomposites are affected by the various dyes, which translate to an effective photosensitization of solar cells. However, optical band gaps of the ZnO–laali and ZnO–zobo shifted towards the red and blue regions, respectively, when compared with that of ordinary ZnO nanoparticle. Consequently, the optical band gaps changed proportionally with shift in absorption edge [29].

Conclusions

In conclusion, we have considered Laali and Zobo (natural dyes) and methyl red (synthetic dye) for the sensitization of ZnO nanoparticle while investigating the optical properties of the hybrid nanocomposites. The natural dyes have been considered because of their good standing photochemical and phototherapeutic applications. Wet chemistry hybridization protocols have been followed which successfully led to inorganic–organic dye nanocomposites (ZnO–laali, ZnO–zobo) as determined by XRD and SEM. There are evidences that isoplumbagin and anthocyanin that are, respectively, present in Laali and Zobo, successfully anchored themselves on ZnO surfaces. In this regard, methyl red behaves differently as a result of its acidic nature which undermined its stability and prevents anchorage. ZnO–laali and ZnO–zobo have demonstrated enhanced absorption and optical properties with evidence of electron injection from the dyes into ZnO scaffold.

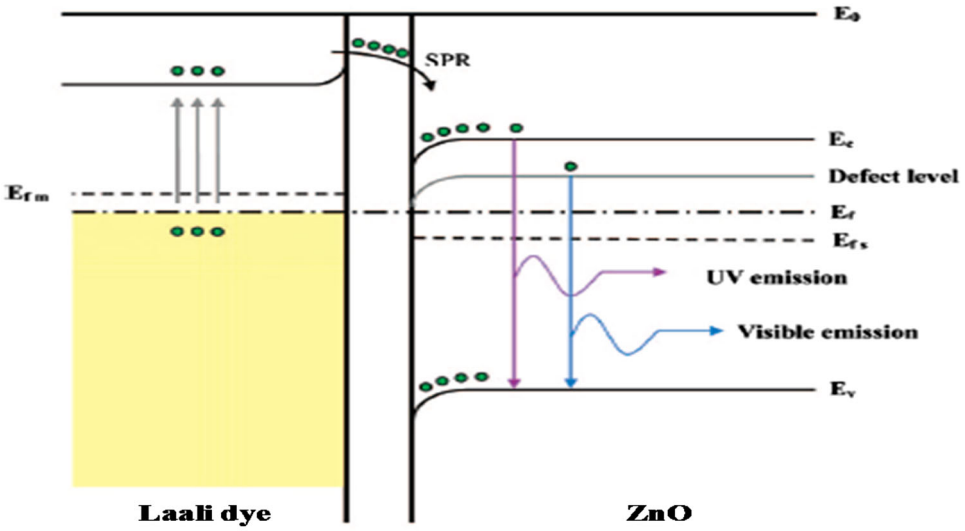

Fig. 6 The energy band structure of a noble metal and ZnO showing the uniform Fermi energy level, induced by electron transfer between the dye and ZnO [27]

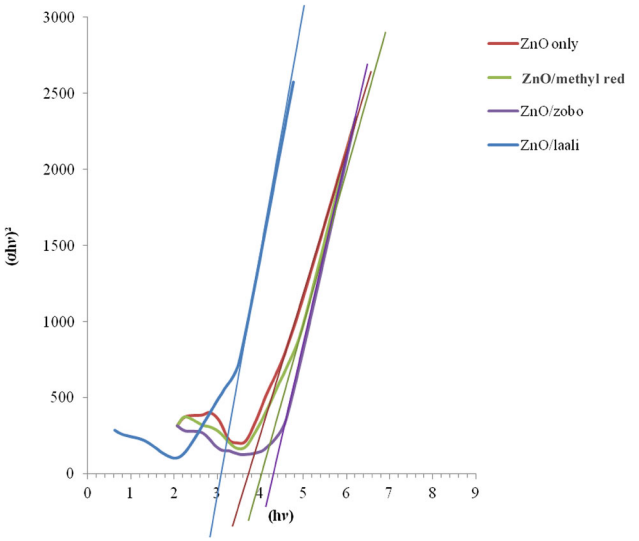

Fig. 7 Plot of $(\alpha hv)^2$ against (hv) for optical band gaps

Contrary phenomenon was displayed by ZnO–methyl red. Overall, by nanoengineering these two materials into a single motif, the ensuing hybrid nanocomposite would not only exhibit the unique properties of dyes and the semiconductor, but also generate novel collective phenomenon based on the interaction of isoplumbagin or anthocyanin with ZnO. Indeed, ZnO–laali, in particular holds a significant promise for application in dye-sensitised solar cells.

References

1. Joshi, S.S., Patil, P.R., Naimase, M.S., Bakare, P.P.: Role of ligands in the formation, phase stabilization, structural and magnetic properties of α-Fe_2O_3 nanoparticles. J. Nanopart. Res. **5**, 635–643 (2006)
2. Cheng, X.L., Zhao, H., Huo, L.H., Gao, S., Zhao, J.G.: ZnO nanoparticulate thin film: preparation, characterization and gas-sensing properties. Sens. Actuators B **102**, 248–252 (2004)
3. Lee, S.Y., Shim, E.S., Kang, H.S., Pang, S.S.: Fabrication of ZnO thin film diode using laser annealing. Thin Solid Films **437**, 31–34 (2005)
4. Wang, Z.L.: Zinc oxide nanostructures: growth properties and applications. J. Phys.: Condens. Matter **16**, R829–R858 (2004)
5. Huang, Y.H., Zang, Y., Liu, L., Fan, S.S., Wei, Y., He, J.: Controlled synthesis and field emission properties of ZnO nanostructures with different morphologies. J. Nanosci. Nanotechnol. **6**, 787–790 (2006)
6. Brida, D., Fortunato, E., Ferreira, I., Aguas, H., Martins, R.: New insights on large area flexible position sensitive detectors. J. Non-Cryst. Solids **299**, 1272–1276 (2002)
7. Suchea, M., Christoulakis, S., Moschovis, K., Katsarakis, N., Kiriakidis, G.: ZnO transparent thin films for gas sensor applications. Thin Solid Films **515**, 551–554 (2006)
8. Chen, J.C., Tang, C.T.: Preparation and application of granular; ZnO/Al_2O_3 catalyst for the removal of hazardous trichloroethylene. J. Hazard. Mater. **142**, 88–96 (2007)
9. Grätzel, M.: Dye-sensitized solar cells. J. Photochem. Photobiol. C **4**, 145–153 (2003)
10. Nazeeruddin, M., Péchy, P., Renouard, T., Zakeeruddin, S., Humphry-Baker, R., Comte, P., Liska, P., Cevey, L., Costa, E., Shklover, V., Spiccia, L., Deacon, G., Bignozzi, C., Grätzel, M.: Engineering of efficient panchromatic sensitizers for nanocrystalline TiO_2-based solar cells. ACS publications. J. Am. Chem. Soc. **123**, 1613–1624 (2001)
11. Longyue, Z., Songyuan, D., Weiwei, X., Kongjia, W.: Dye-sensitized solar cells based on ZnO films. Plasma Sci. Technol. **8**, 172–175 (2006)
12. Bmer, C., Boschloo, G., Hagfeld, A.: Electron injection and recombination in Ru(dcbpy)2(NCS)2 sensitized nanostructured ZnO. J. Phys. Chem. B **105**, 5585–5588 (2001)
13. Hara, K., Horiguchi, T., Kinoshita, T., Sayama, K., Arakawa, H.: Solar energy mater. Solar Cells **64**, 115 (2000)
14. Ito, S., Saitou, T., Imahori, H., Ueharad, H., Hasegawa, N.: Fabrication of dye-sensitized solar cells using natural dye for food pigment: *Monascus yellow*. Energy Environ. Sci. **3**, 905–909 (2010)
15. Boyo, A.O., Boyo, H.O., Abdusalam, I.T., Adeola, S.: Dye Sensitized nanocrystaline titania solar cell using laali stem bark (*lawsonia inermis*). Transl. J. Sci. Tech. **2**, 60 (2012)
16. Ukwubile, C.A., Otalu, O., Babalola, B.J.: Comparative colour stabilization of Zobo (*Hibiscus sabdarifa*) drink containing anthacyanin pigment. J. Poisonous Med. Plants Res. **21**, 16–19 (2013)
17. Ann, Mary: Anthocyanins and human health: an in vivo investigative approach. J. Biomed. Biotech. **5**, 306–313 (2004)
18. Adenike, O.B., Henry, O.B., Ibrahim, T.A.: Dye sensitized nanocrystaline titania solar cell using laali stem bark (*Lawsonia inermis*). Transnal. J. Sci. Technol. **2**(4), 60–72 (2009)
19. Olowosulu, A.K., Akpa, P.A., Eze, U.V., Adikwu, M.U.: Spectrophotometric analysis of *Hibiscus sabdariff*a colourant at different pH values Nig. J. Pharm. Sci. **7**, 36–40 (2008)
20. Taher, M., El-Agez, Ahmed, A., El-Tayyan, Al-Kahlout, A., Sofyan, A., Taya, M., Abdel-Latif, S.: Dye-sensitized solar cells based on ZnO films and natural dyes. J. Mater. Chem. **2**, 105–110 (2012)
21. Olea, A., Ponce, G., Sebastian, P.J.: Electron transfer via organic dyes for solar conversion. Sol. Energy Mater. Sol. Cells **59**(1), 137–143 (1999)
22. McDougall, G.J., Fyffe, S., Dobson, P., Stewart, D.: Anthocyanins from red cabbage—stability to simulated gastrointestinal digestion. Phytochemistry **68**, 1285–1294 (2007)
23. Buraidah, M. H., Teo, L. P., Yusuf, S. N. F., Noor, M. M., Kufian, M. Z., Careem, M. A., Majid, S. R., Taha, R. M., Arof1 A. K.: TiO_2/Chitosan-NH_4I(+I2)-BMII-based dye-sensitized solar cells with anthocyanin dyes extracted from black rice and red cabbage. Int. J. Photoenergy. **2011** (2011). doi:10.1155/2011/273683
24. Qifeng, Z., Christopher, S., Dandeneaw, S., Xiaoyuan, Z., Guozhang, C.: ZnO nanostucture for dye-sensitized solar cells. Adv. Mater. **21**, 4087 (2009)
25. Zhang, Q.: Effects of Lithium ions on dye-sensitize ZnO aggregate solar cells. Chem. Mater. **22**, 2427–2433 (2010)
26. Lee, M.K., Kim, T.G., Kim, W., Sung, Y.M.: Surface plasmon resonance (SPR) electron and energy transfer in noble metal-zinc oxide composite nanocrystals. J. Phys. Chem. C **112**, 10079–10082 (2008)

27. Rayleigh, L.: On the light from the sky, its polarization and colour. Philos. Mag. **41**, 107, 274 (1871)
28. Jain, A., Sagar, P., Mehra, R.: Band gap widening and narrowing in moderately and heavily doped n-ZnO films. Solid State Electron. **50**, 1420–1424 (2006)
29. Kim, S., Nam, G., Park, H., Yoon, H., Lee, S.-H., Kim, J.S., Kim, J.S., Kim, D.Y., Kim, S.-O., Leem, J.-Y.: Effects of doping with Al, Ga, and In on structural and optical properties of ZnO nanorods grown by hydrothermal method. Bull. Korean Chem. Soc. **34**, 1205–1211 (2013)